

Differential scanning fluorimetry as secondary screening platform for small molecule inhibitors of Bcl-X_L

Kah Fei Wan,¹ Sifang Wang,¹ Christopher J. Brown,² Victor C. Yu,² Michael Entzeroth,¹ David P. Lane^{1,2} and May Ann Lee^{1,*}

¹Experimental Therapeutics Center (ETC); and ²Institute Molecular and Cell Biology (IMCB); A*STAR; Biopolis, Singapore

Key words: differential scanning fluorimetry, Bcl-X_L inhibitors, fluorescence polarization, secondary screening, glutathione-S-transferase

Abbreviations: HTS, high-throughput screening; DSF, differential scanning fluorimetry; GST, glutathione S-transferase; NMR, nuclear magnetic resonance; T_m, melting temperature; RFU, relative fluorescence unit

Since apoptosis is impaired in malignant cells overexpressing prosurvival Bcl-2 proteins, drugs mimicking their natural antagonists, BH3-only proteins, might overcome chemoresistance. Small molecule inhibitors of Bcl-X_L function have been discovered from diverse structure classes using rational drug design as well as high-throughput screening (HTS) approaches. However, most of the BH3 mimetics that have been identified via screening based on fluorescence polarization displayed an affinity for their presumed protein targets that is far lower than that of BH3-only proteins. Therefore, it is important to establish a simple and inexpensive secondary platform for hit validation which is pertinent to current efforts for developing compounds that mimic the action of BH3-only proteins as novel anticancer agents. These considerations prompted us to explore the differential scanning fluorimetry (DSF) method that is based on energetic coupling between ligand binding and protein unfolding. We have systematically tested known Bcl-X_L/Bcl-2 inhibitors using DSF and have revealed distinct subsets of inhibitors. More importantly, we report that some of these inhibitors interacted selectively with glutathione S-transferase tagged Bcl-X_L, whereas certain inhibitors exhibited marked selectivity towards native untagged Bcl-X_L. Therefore, we propose that the affinity tag may cause a significant conformational switch in the Bcl-X_L, which results in the selectivity for certain subsets of small molecule inhibitors. This finding also implies that the previous screens involving tagged proteins need to be carefully reexamined while further investigations must ensure that the right conformation of protein is used in future screens.

Introduction

Proteins of the Bcl-2 family are the central transducers of survival and apoptotic signals. They act on the mitochondria by regulating the permeability and integrity of the mitochondrial outer membranes, thereby controlling the release of apoptogenic factors. The Bcl-2 family consists of three major subfamilies of pro-survival and pro-apoptotic molecules. Members of BH3-only subfamily (Bim, Bad, Bid, Bik, Noxa, Puma and Hrk) serve as sentinels for the initiation of apoptosis by modulating the function of members of the other two multi-domain pro-survival (Bcl-2, Bcl-w, Mcl-1, Bcl-X_L and A1/Bfl-1) or pro-apoptotic (Bax and Bak) subfamilies.¹⁻⁴ Overexpression of the pro-survival Bcl-2 family proteins occurs in many cancers, generating interest in these proteins as possible drug discovery targets.⁵ A favored strategy for Bcl-2 antagonism is based on mimicking the action of endogenous inhibitors that bind Bcl-2 and related proteins.⁶ Several small molecule inhibitors of the Bcl-2 family have already been identified and reported to occupy the same binding site

on Bcl-2 or Bcl-X_L as the BH3 peptide, promoting apoptosis. These chemical inhibitors of Bcl-2 and Bcl-X_L are now commonly employed as research tools for interrogating the function of pro-survival Bcl-2 family proteins, and some may enter human clinical trial as potential cancer treatments. Included among these BH3-mimicking chemical antagonists of Bcl-2/Bcl-X_L are the natural products gossypol, epigallocatechin, chelerythrine, kandomycin and antimycin A, which bind Bcl-2 and Bcl-X_L with micromolar affinities, measured by competitive BH3 peptide displacement assays.⁷⁻¹² Another promising candidate developed using NMR based screening and intense synthetic chemistry efforts is ABT-737, which was first synthesized by Abbott Laboratories, it is by far the most potent current inhibitor (K_d ~1 nM for Bcl-2 and Bcl-X_L).¹³

One of the major challenges for the development of Bcl-2 small molecule inhibitors that disrupts protein-protein interaction is the failure to ensure that the optimal region of compound space is being screened or that the compounds that are found can be easily optimized for these diverse interfaces.¹⁴ In

*Correspondence to: May Ann Lee; Email: malee@etc.a-star.edu.sg

Submitted: 09/16/09; Accepted: 09/17/09

Previously published online: www.landesbioscience.com/journals/cc/article/10114

several examples, the BH3 mimetics that have been identified via high-throughput screening (HTS) involving natural product libraries based on fluorescence polarization, displayed an affinity for their presumed protein targets that is far lower than that of BH3-only protein.^{9,15} Extensive biophysical techniques were also followed to check that the hit compounds were 'real' and stoichiometric before proceeding with investment in medicinal chemistry approaches. Therefore, developing secondary platforms to rapidly identify and eliminate promiscuous binders is crucial to the goal of providing high quality candidate compounds for lead optimization activities.

Here, we describe using the differential scanning fluorimetry (DSF) method for rapid and inexpensive secondary screening to identify Bcl-2 small molecule inhibitors that bind and stabilize purified Bcl-X_L.¹⁶ Bcl-X_L proteins were subjected to gradually increasing temperature, and the temperature shift between the melting temperature (T_m) in the presence and absence of inhibitors were measured.¹⁶ The extent of temperature shift is believed to be proportional to the affinity of the inhibitors. We also sought to expand our understanding of the interactions by comparing the Glutathione S-transferase (GST)-tagged Bcl-X_L (GST-Bcl-X_L) and untagged Bcl-X_L (Bcl-X_L) proteins. We selected known BH3 peptides and Bcl-2/Bcl-X_L inhibitors for characterization of their stabilization and binding to these proteins. A majority of these inhibitors bind and stabilize the GST-tagged Bcl-X_L, an expected observation obtained from fluorescence polarization assay. To our surprise, we found that some of these inhibitors fail to stabilize untagged Bcl-X_L, thereby revealing distinct subsets of inhibitors. We have also further delineated this observation using both proteolytic trypsin digestion and fluorescence polarization approaches. Even more surprising was the observation that ABT-737 while potently active in stabilizing untagged Bcl-X_L was not active when tested against the GST-tagged protein.

Results

Protein-peptide interactions of Bcl-2 family members by DSF method. Numerous techniques have been introduced for measuring the binding affinity of Bcl-2 small molecule inhibitors. Many of these tools such as chemical perturbations, surface plasmon resonance and nuclear magnetic resonance (NMR) lack robustness and generality, thereby requiring significant development time. Fluorescence polarization-based screening has been widely used to monitor the ability of small molecule inhibitors to displace fluorochrome-conjugated BH3 peptides from Bcl-2 pro-survival family proteins, due to its unique combination of homogeneity, simplicity, speed and robustness.¹⁷ However, being a ratiometric technique, fluorescence polarization is sensitive to protein denaturing agents and to absorbance and color quenching especially from auto-fluorescent natural library compounds, and these effects could result in false positive.¹⁷ Furthermore, most of these compounds reported to be active in these assays have shown little relationship between structure and function, and much work has been devoted to identifying and understanding these enigmatic molecules. Therefore, these considerations prompted us to explore DSF method as a secondary platform to eliminate

promiscuous binders and protein denaturants from the screens. DSF monitors thermal unfolding and stability of proteins in the presence of a fluorescent dye, and ligand-induced perturbations in thermal stability are observed as a change in the protein melting temperature (T_m).¹⁶ Two types of Bcl-X_L proteins, one with a GST-tag and the other with GST-cleaved off by thrombin, were examined. We first assessed whether the T_m of these proteins could be measured reproducibly and with thermal envelopes that conformed to the prototypical melting transitions. The fluorescence intensity (RFU) was plotted as a function of temperature; this generates a sigmoidal shape that can be described by a two-state transition (Fig. 1A and B). The unfolding transition for both GST-Bcl-X_L and Bcl-X_L were indicated by an increase in fluorescence, which is due to the increase binding of the Sypro Orange dye to the exposed hydrophobic regions of the unfolded proteins. Following the peak in the intensity, the fluorescence intensity started to decrease, probably due to aggregation of the denatured protein-dye complexes (Fig. 1A and B). By fitting the fluorescence intensity to Boltzmann equation, the melting temperature of GST-Bcl-X_L (T_m = 52.92 ± 0.04°C) was obtained as the point of inflection of the melting curve (Fig. 1A). Untagged Bcl-X_L has better stability compared to GST-Bcl-X_L, unfolding at T_m = 70.35 ± 0.08°C (Fig. 1B). This compared well with the T_m determined by differential scanning calorimetry.¹⁸ Noteworthy, both proteins showed sharp two-state melting transitions even though there were multi-domain proteins, suggesting a cooperative unfolding of these proteins due to energetic coupling between the domains. The observed T_m values for both proteins are highly reproducible, with a standard deviation of <0.1°C determined for the same batch of protein from up to 10 repeat measurements. For different batches of proteins, the absolute values for T_m often differed by a few degree (<2°C), which depends mainly on the protein preparation (e.g., variability in proteins concentration estimation) and instrumentation.

Next, we assessed the effect of Bak BH3 peptide on the T_m of GST-Bcl-X_L and Bcl-X_L, as our previous fluorescence polarization-based HTS were performed using fluorochrome-conjugated Bak BH3 peptide.⁹ We found that the Bak BH3 peptide increased the thermal stability of Bcl-X_L and GST-Bcl-X_L, and the resulting ΔT_m determined for Bcl-X_L (+1.97°C) compared well with GST-Bcl-X_L (+1.34°C) (Fig. 1A and B), suggesting that GST does not significant affect the binding of Bak BH3 peptide towards Bcl-X_L. Other BH3 peptides were also tested by DSF. Bad and Puma BH3 peptides increased the thermal stability of GST-Bcl-X_L and Bcl-X_L, whereas Noxa had little effect on the thermal stability of these proteins (Fig. 1C). This is consistent with prior studies showing that Bad and Puma bound tightly to Bcl-X_L, but not Noxa that binds selectively only to Mcl-1.¹⁹ The variability of the assay (<0.1°C) was much smaller than the temperature shift (ΔT_m >1°C), indicating the significance of the small T_m shift that are observed for the binding of the peptides to the proteins. Collectively, our data indicate that DSF serves as a valid platform to study the protein-peptide interactions of Bcl-2 family members.

DSF to study protein-drug interactions of Bcl-2 family members. DSF was then used to profile various known Bcl-2/

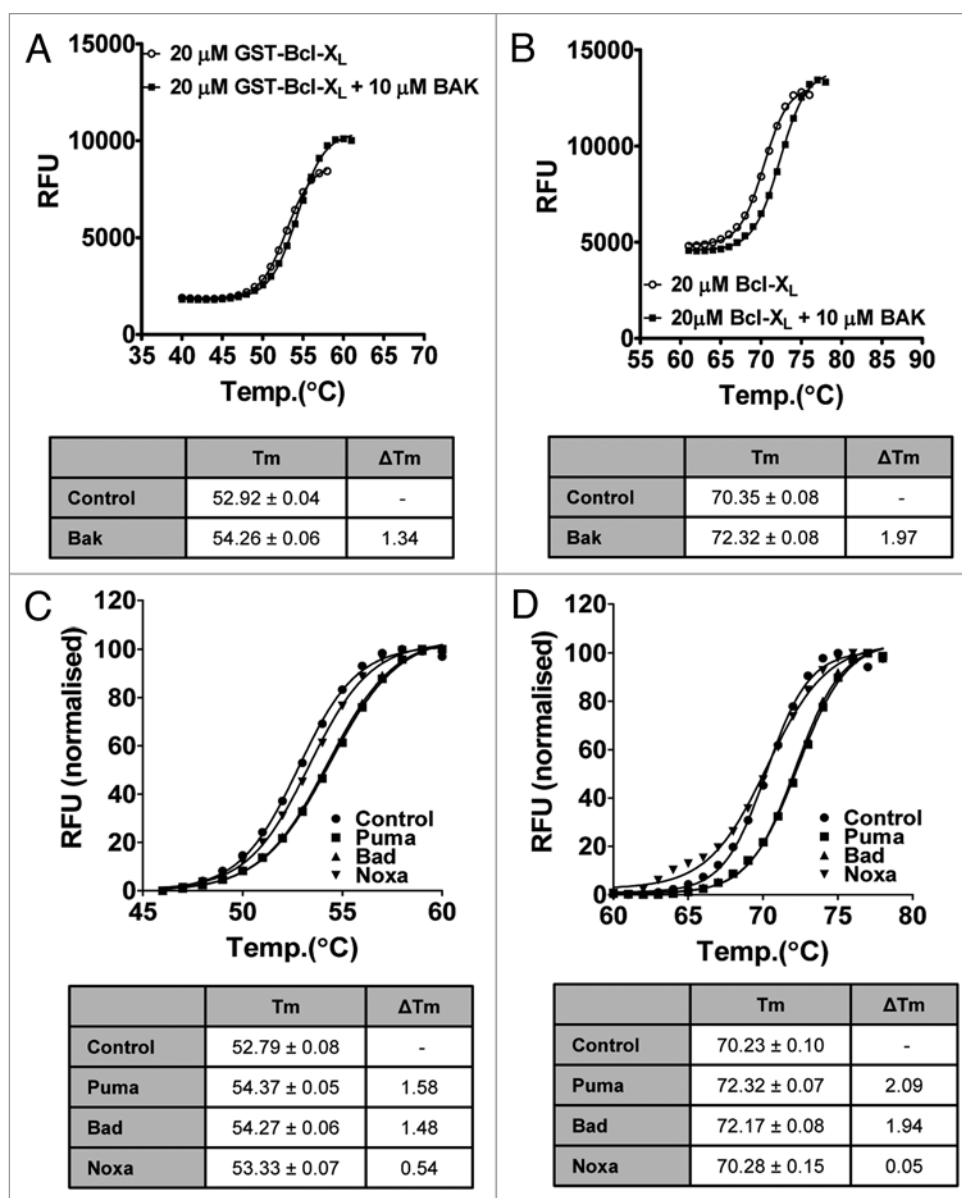


Figure 1. The effect of BH3 peptides on melting temperature (T_m) of (A and C) GST-Bcl-X_L and (B and D) Bcl-X_L measured by DSF. (A and B) Reaction mixtures contained Sypro orange and 20 μ M proteins in the presence or absence of 10 μ M Bak BH3 peptides (BAK). RFU was plotted as a function of temperature for (A) GST-Bcl-X_L and (B) Bcl-X_L. Integrated intensity from reactions was fitted to Boltzmann equation as described in Materials and Methods to obtain the melting temperature T_m . (C and D) Normalized RFU was plotted as function of temperature for (C) GST-Bcl-X_L and (D) Bcl-X_L in the absence (control) or presence of Bad, Puma and Noxa BH3 peptides. RFU: relative fluorescent units. BH3 peptides sequences = Bak (GQVGRQLAIIGDDINR); Bad (NLWAAQRYGRELRRMSDEFVDSFKKG); Puma (EEQWAREIGAQLRRMAD-DLNAQYERR); hNoxa (PAELEVEC-ATQLRRFGDKLNFRQKLL). Data are representative of at least three experiments.

Bcl-X_L inhibitory compounds against GST-Bcl-X_L (Fig. 2A) and Bcl-X_L (Fig. 2B). Table 1 summarizes the result for known Bcl-2/Bcl-X_L inhibitors kendomycin, BH3I-1, BH3I-2, HA14-1, YC-137, epigallocatechin (EGCG), chelerythrine, gossypol, ABT-737 and its enantiomer tested at a single concentration of 100 μ M.^{7-10,12,13,20-23} Kendomycin, which was recently identified by us from the fluorescence polarization-based HTS of natural product libraries, gave the highest ΔT_m value (+11.74°C) in GST-Bcl-X_L (Fig. 2A), but only caused +1.87°C shift in T_m of Bcl-X_L (Fig. 2B). To our surprise, ABT-737, which is the most potent antagonist of Bcl-X_L reported to date, selectively increased T_m

of Bcl-X_L by +14.74°C (Fig. 2B), but not GST-Bcl-X_L ($\Delta T_m = +0.55^\circ\text{C}$; Fig. 2A). Enantiomer of ABT-737 caused a marginal increase in T_m for Bcl-X_L ($\Delta T_m = +6.74^\circ\text{C}$; Fig. 2B), which is consistent with other studies showing that this analogue of ABT-737 shares weaker activity. Similar to ABT-737, the enantiomer failed to cause any shift in T_m for GST-Bcl-X_L. Interestingly, the majority of the known Bcl-X_L/Bcl-2 inhibitors selectively exhibited thermal stability activities towards GST-Bcl-X_L (Fig. 2A), but failed to have any positive ΔT_m towards Bcl-X_L (Fig. 2B). Noteworthy, chelerythrine and its homologues sanguinarine potentially increased the T_m of GST-Bcl-X_L (Fig. 2A), whereas a

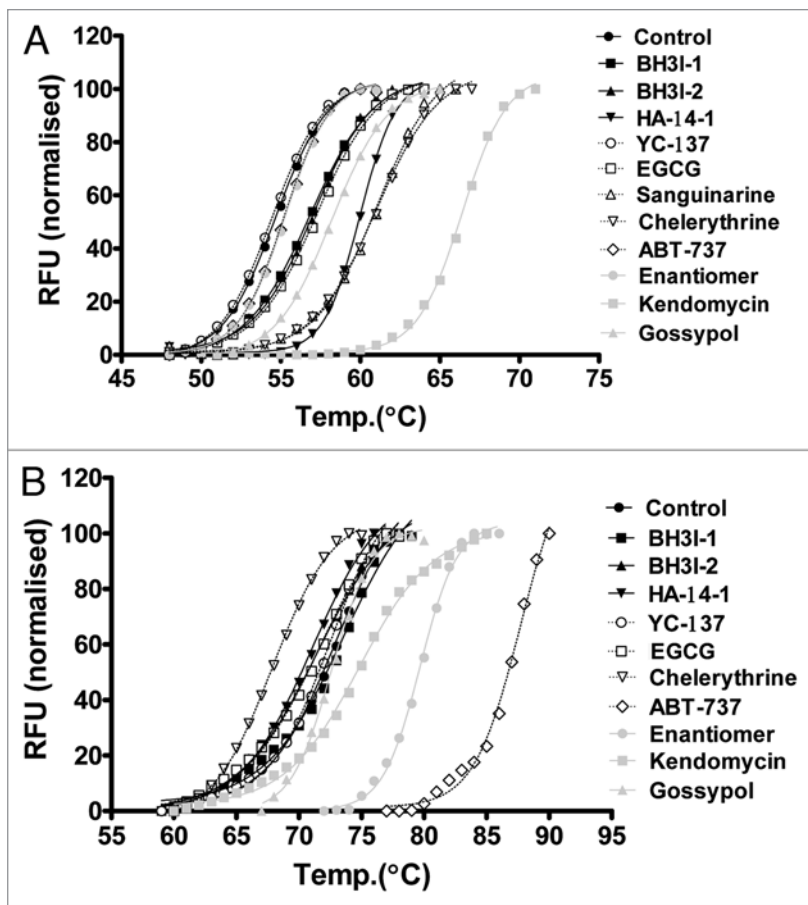


Figure 2. The effect of Bcl-X_L/Bcl-2 inhibitors on melting temperature (T_m) of (A) GST-Bcl-X_L and (B) Bcl-X_L measured by DSF. Normalized RFU was plotted as function of temperature for 20 μM of (A) GST-Bcl-X_L and (B) Bcl-X_L in the absence (control) or presence of 100 μM Bcl-2/Bcl-X_L inhibitor. Data are representative of at least three experiments.

negative ΔT_m of Bcl-X_L was observed suggestive that these compounds caused a decrease in stability due to a more disordered conformation (Fig. 2B). YC-137 failed to have any effect on both proteins by DSF, which is consistent with other observation that YC-137 preferentially binds to Bcl-2 protein.²⁰ As controls for our DSF analysis, we have tested several non-Bcl-2/Bcl-X_L inhibitory compounds such as etoposide (topoisomerase inhibitor) and nutlin-3 (Mdm2 inhibitor) as negative controls, and none of these compounds have any activity on either protein by DSF (data not shown). We have excluded the non-specific effect of these inhibitors towards GST-only protein as these inhibitors failed to affect the T_m of GST proteins (Table 1). Taken together, our results reveal the distinct binding patterns of these antagonists towards GST-Bcl-X_L and Bcl-X_L. More importantly, the spectrum of DSF activities of the chemical inhibitors indicates that there are 4 classes of Bcl-X_L/Bcl-2 inhibitors: (1) ABT-737 and its enantiomer selectively target Bcl-X_L; (2) Kendomycin targets GST-Bcl-X_L preferably over Bcl-X_L; (3) Chelerythrine and others target potently towards GST-Bcl-X_L but caused destabilization

towards Bcl-X_L; (4) YC-137 had no effect towards both types of Bcl-X_L proteins.

As the previous result was obtained with a single high concentration of compounds, we sought to expand our DSF analysis by evaluating a range of concentrations of the compounds with respect to their ability to increase T_m of proteins from binding. Some of the examples of the dose-dependent melting curve with 2 fold serial dilution of the different classes of inhibitors are shown in Figure 3. Kendomycin increased the thermal stability of GST-Bcl-X_L in a concentration-dependent manner (Fig. 3A; right), whereas there was absence of dose-dependent effect observed with Bcl-X_L (Fig. 3A; left). We have excluded the possibility that this phenomenon is due to the intrinsic fluorescence of kendomycin, as we failed to observe any unfolding transition in the absence of Sypro Orange dye (data not shown). Chelerythrine exhibited a dose-dependent positive and negative ΔT_m in GST-Bcl-X_L (Fig. 3B; right) and Bcl-X_L (Fig. 3B; left) respectively. In contrast, ABT-737 caused a dramatic thermal shift on Bcl-X_L (Fig. 3C; left), but had minimal effect on GST-Bcl-X_L (Fig. 3C; right). The increases in the thermal stability, ΔT_m , as a function of concentration of different classes of inhibitors are shown in Figure 3D.

Proteolytic digestion analysis of GST-Bcl-X_L and Bcl-X_L. To further verify the DSF findings, we examined whether these compounds could affect the susceptibility of the recombinant GST-Bcl-X_L and Bcl-X_L to non-specific proteases, such as trypsin. We assumed that the proteins must unfold to become accessible to trypsin proteolytic digestion, which is reminiscent to DSF that monitors the thermal unfolding of these proteins. Trypsin was found to cleave GST-Bcl-X_L (50 kDa) to 27 kDa, 26 kDa and 23 kDa fragments (Fig. 4A; control), whereas proteolysis of Bcl-X_L (26 kDa) produced only one <20 kDa fragment (Fig. 4B; control). We found that the proteolysis of Bcl-X_L occurred at much slower kinetics (2 h) compared to GST-Bcl-X_L (5 min) (Fig. 4A and B, data not shown), which correlated well with the better thermal stability of Bcl-X_L in DSF. Similar to DSF, kendomycin, chelerythrine, sanguinarine, HA14-1 and gossypol remained as the most potent inhibitors in protecting GST-Bcl-X_L from trypsin proteolysis (Fig. 4A and C), whereas ABT-737 and its enantiomer appeared to be less effective in blocking the effect of trypsin digestion on GST-Bcl-X_L (Fig. 4A). In contrast, Bcl-X_L was well protected from trypsin digestion by ABT-737 and its enantiomer, but not by other known inhibitors (Fig. 4B). Consistent with other observations, YC-137 failed to have any protective effect towards GST-Bcl-X_L and Bcl-X_L (Fig. 4A and B). We have also excluded the non-specific effect of these inhibitors in inhibiting trypsin activity, since these inhibitors failed to affect the proteolysis of GST-only protein (data not shown).

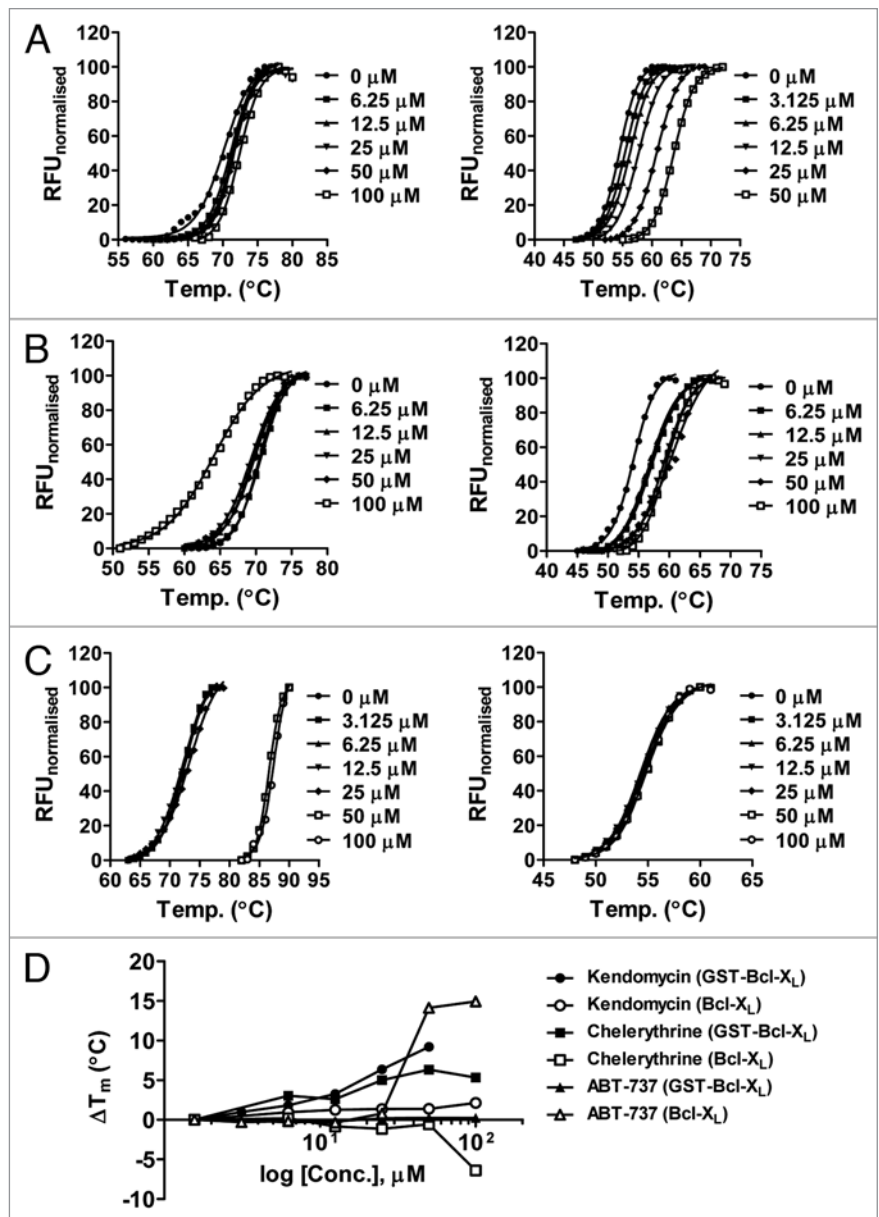
Table 1. Summary table of T_m and ΔT_m for known Bcl-X_L/Bcl-2 inhibitors

Bcl-X _L /Bcl-2 inhibitors	GST-only		GST-Bcl-X _L		Bcl-X _L	
	T_m	ΔT_m	T_m	ΔT_m	T_m	ΔT_m
Control	54.66 ± 0.06	-	54.66 ± 0.06	-	72.94 ± 0.27	-
ABT-737	55.60 ± 0.3	-0.04	55.21 ± 0.06	+0.55	87.68 ± 0.44	+14.74
Enantiomer	55.28 ± 0.5	-0.36	54.27 ± 0.05	+0.61	79.68 ± 0.10	+6.74
Kendomycin	55.38 ± 0.7	-0.26	66.40 ± 0.07	+11.74	74.82 ± 0.13	+1.87
Chelerythrine	54.61 ± 0.5	-1.03	60.98 ± 0.08	+6.32	67.86 ± 0.09	-5.08
HA14-1	55.89 ± 0.6	+0.20	59.98 ± 0.05	+5.32	71.01 ± 0.21	-1.93
Gossypol	54.78 ± 0.6	-0.87	58.20 ± 0.03	+3.54	72.61 ± 0.13	-0.33
BH31-1	54.89 ± 0.6	-0.75	56.84 ± 0.04	+2.18	73.52 ± 0.46	+0.58
BH31-2	55.42 ± 0.7	-0.22	57.05 ± 0.12	+2.39	71.38 ± 0.21	-1.56
EGCG	55.16 ± 0.5	-0.48	57.27 ± 0.08	+2.61	71.63 ± 0.30	-1.31
YC-137	54.55 ± 0.5	-1.09	54.41 ± 0.05	-0.25	72.47 ± 0.23	-0.47

Figure 3. Dose-response studies of Bcl-X_L/Bcl-2 inhibitors by DSF. (A–C) Thermostability of Bcl-X_L (left) and GST-Bcl-X_L (right) in the presence of indicated concentrations of (A) kendomycin; (B) chelerythrine; (C) ABT-737 measured by DSF. Normalized RFU was plotted as function of temperature. (D) The increases in the thermal stability, ΔT_m , as a function of concentration of Bcl-X_L/Bcl-2 inhibitors are shown. Data are representative of at least three experiments.

Next, we examined whether these compounds prevent trypsin digestion in a dose-dependent manner. GST-Bcl-X_L was protected from trypsin proteolysis by kendomycin in a dose-dependent manner, and it exhibited better potency as compared to ABT-737 (Fig. 4C). The reverse was observed with Bcl-X_L, in which ABT-737, but not kendomycin potently inhibited the trypsin proteolysis of Bcl-X_L (Fig. 4D). These data indicate a good correlation between DSF and proteolysis analysis, further supporting the general applicability of ligand-induced conformational stabilization of proteins as useful tool for secondary screening strategy.

Fluorescence polarization assay of GST-Bcl-X_L and Bcl-X_L. Most of the reported HTS for small molecule inhibitors of Bcl-X_L/Bcl-2 were performed in fluorescence polarization-based competitive binding assay using tagged Bcl-2 family members (Table 2). Most of the known Bcl-2/Bcl-X_L inhibitors were reported to have low micromolar activities, and ABT-737 remained as the most potent inhibitor that displays nanomolar activity in fluorescence polarization assay (Table 2). The slight difference in IC₅₀ of these compounds as compared



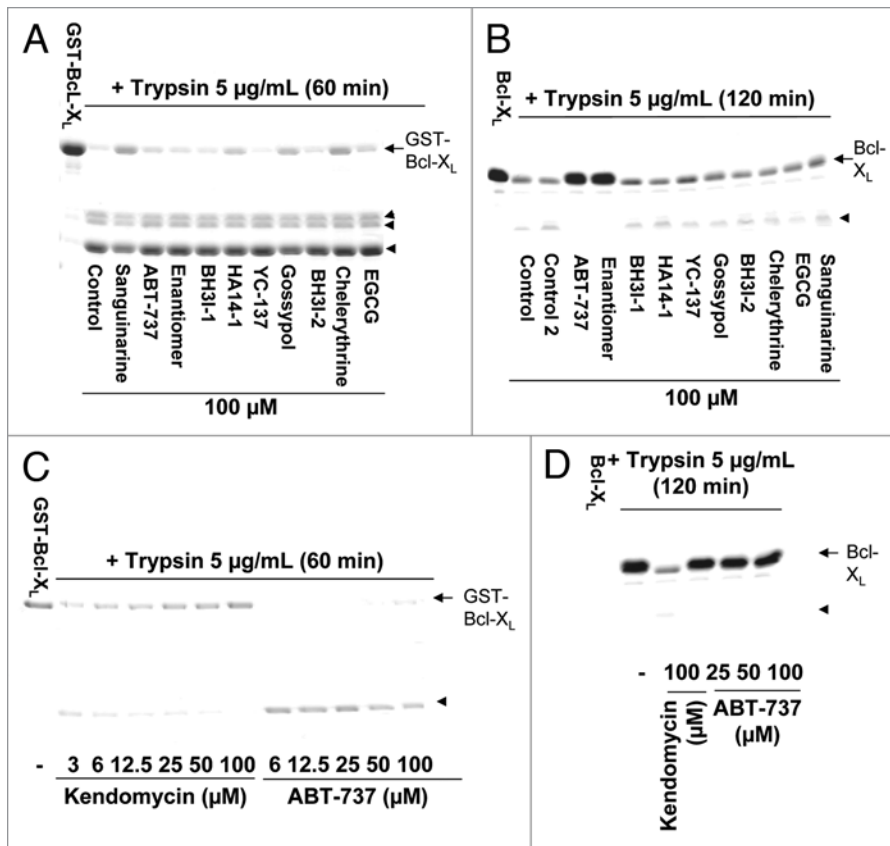


Figure 4. Trypsin digestion analysis of (A and C) GST-Bcl-X_L and (B and D) Bcl-X_L upon Bcl-X_L/Bcl-2 inhibitors treatment. (A and B) 0.5 mg/mL GST-Bcl-X_L (A) or Bcl-X_L (B) were incubated with trypsin (5 µg/mL) at 4°C in the absence (control) and presence of 100 µM Bcl-X_L/Bcl-2 inhibitors for the indicated durations. Native proteins (GST-Bcl-X_L = 50 kDa; Bcl-X_L = 26 kDa) in the absence of trypsin proteolysis was loaded into the first lane of the coomassie stained-gel as negative control. Arrows indicate cleaved fragments. (C and D) 0.5 mg/mL GST-Bcl-X_L (C) or Bcl-X_L (D) were incubated with the indicated doses of kendomycin or ABT-737 in the presence of trypsin (5 µg/mL) at 4°C for the indicated durations. Native proteins (GST-Bcl-X_L = 50 kDa; Bcl-X_L = 26 kDa) in the absence of trypsin proteolysis was loaded as negative control. Arrows indicate cleaved fragments. Data are representative of at least three experiments.

to the reported value is probably due to the use of different BH3 peptides with different affinities for Bcl-X_L, particularly if of higher affinity than the Bak BH3 peptide employed here. However, our finding implies that the previous screens involving tagged Bcl-2 family members may need to be carefully re-examined. In this instance, we have sought to compare the displacement of Bak BH3 peptide from GST-Bcl-X_L and Bcl-X_L by fluorescence polarization assay. FAM-labeled Bak BH3 peptides bound to both Bcl-X_L and GST-Bcl-X_L in a concentration-dependent and saturable manner (Fig. 5A). Binding of the FAM-labeled BH3 peptides were competed from both proteins by unlabeled Bak BH3 peptides, confirming the competitive and reversible binding (Fig. 5B). The relative competitive affinities (IC₅₀) against GST-Bcl-X_L and Bcl-X_L were 29 µM and 11 µM respectively, and this is consistent with the slightly higher T_m shift of the peptides towards the Bcl-X_L (ΔT_m = +1.97°C) as compared to GST-Bcl-X_L (ΔT_m = +1.34°C). However, our re-investigation of those compounds using untagged Bcl-X_L in fluorescence polarization assay

revealed most of these compounds were semi-selective antagonists that displayed better inhibitory activities towards GST-Bcl-X_L instead of Bcl-X_L (Fig. 5; Table 3). Bak BH3 peptide was displaced more efficiently from GST-Bcl-X_L than Bcl-X_L by chelerythrine (>50 fold; Fig. 5C) and kendomycin (8 fold; Fig. 5D). BH3I-1, BH3I-2 and gossypol also displayed slightly better inhibitory activities towards GST-Bcl-X_L as compared to Bcl-X_L (~ 2 fold; Fig. 5E; Table 3). Noteworthy, BH3I-2 exhibited a much lower inhibitory efficacy in Bcl-X_L (minimal mp = 180) than GST-Bcl-X_L (minimal mp = 90) (Fig. 5E). Strikingly, ABT-737 displayed similar affinities to both GST-Bcl-X_L and Bcl-X_L (Fig. 5F), which appeared to be distinct from DSF profiles (Fig. 3C). As negative control, YC-137 remained inactive in displacing Bak BH3 peptide from Bcl-X_L (Table 3). Together, the fluorescence polarization results raise the possibility that the affinity tag may cause a significant conformational change in the Bcl-X_L, thereby results in the selectivity for certain subsets of small molecule inhibitors towards GST-Bcl-X_L. More importantly, the distinct profiles between DSF and fluorescence polarization assay for ABT-737 indicate that DSF could serve as valuable tool in hits selection which may otherwise be masked in fluorescence polarization assays.

Discussion

In this study we have systematically compared the binding activities of BH3 peptides and known chemical inhibitors of Bcl-2 family members in affinity-tagged Bcl-X_L and untagged Bcl-X_L measured by fluorescence anisotropy-based DSF and FPA. We reported that although BH3 peptides exhibited no difference in binding for GST-Bcl-X_L and Bcl-X_L, the spectrum of DSF activities of the chemical inhibitors revealed several classes of antagonists, which interestingly exhibited preferences in binding towards affinity-tagged Bcl-X_L or untagged Bcl-X_L. This is contrary to previous expectations that GST does not significant affect the results of fluorescence polarization assays.²⁴ In fact, the distinctive DSF profile observed with ABT-737 was particularly striking, as the results with DSF were not concordant with those obtained by fluorescence polarization assay. ABT-737 displayed similar affinities to both GST-Bcl-X_L and Bcl-X_L measured by fluorescence polarization assay, whereas DSF failed to report any activity of this compound towards GST-Bcl-X_L. More pertinently, their binding profiles contrast sharply with the behavior of other known inhibitors. The opposite activities of other known antagonists towards

Table 2. Summary table of reported potency of known Bcl-X_L/Bcl-2 inhibitors

Inhibitors	FPA Activity	Conditions for FPA
Kendomycin ¹²	IC ₅₀ = 12.3 μM	<ul style="list-style-type: none"> Protein: GST-Bcl-X_L Peptide: Bak BH3 peptide (Flu-KGGGQVGRRLAIIGDDINR)
Chelerythrine ⁹	IC ₅₀ = 1.5 μM	<ul style="list-style-type: none"> Protein: GST-Bcl-X_L Peptide: Bak BH3 peptide (Flu-KGGGQVGRRLAIIGDDINR)
YC-137 ²⁰	Ki = 1.3 μM	<ul style="list-style-type: none"> Protein: His6-Bcl-2 Peptide: 6-carboxy fluorescein succinimidyl ester Bid peptide (Flu-QEDIIRNIARHLAQVDGDSMDR)
HA14-1 ²³	IC ₅₀ = 9 μM	<ul style="list-style-type: none"> Protein: GST-Bcl-2 Peptide: 5-carboxyfluorescein Bak BH3 peptide (Flu-GQVGRQLAIIGDDINR)
BH3I-1 ²²	Ki = 2.4 μM	<ul style="list-style-type: none"> Protein: GST/His6-Bcl-X_L Peptide: Oregon Green Bak BH3 peptide (KGGGQVGRRLAIIGDDINR)
BH3I-2 ²²	Ki = 4.1 μM	<ul style="list-style-type: none"> Protein: GST-Bcl-X_L Peptide: Oregon Green Bak BH3 peptide (KGGGQVGRRLAIIGDDINR)
Gossypol ⁷	IC ₅₀ = 0.4 μM (Bcl-X _L) 10 μM (Bcl-2)	<ul style="list-style-type: none"> Protein: GST-Bcl-X_L/Bcl-2 Peptide: 5-carboxyfluorescein Bak BH3 peptide (Flu-GQVGRQLAIIGDDINR)
EGCG ⁸	Ki = 490 nM (Bcl-X _L) 335 nM (Bcl-2)	<ul style="list-style-type: none"> Protein: Bcl-X_L/Bcl-2 Peptide: FITC Bad BH3 peptide (NL-WAAQRYGRELRRMSD-K(FITC)-FVD)
ABT-737 ²⁴	IC ₅₀ = 64 nM (Bcl-X _L) 120 nM (Bcl-2)	<ul style="list-style-type: none"> Protein: GST-Bcl-X_L/Bcl-2 Peptide: FITC-Bid BH3 peptide (FITC-Ahx-EDIIRNIARHLAQVDGDSMDR)

untagged Bcl-X_L were unraveled by DSF, but not by fluorescence polarization assay, further supporting the latter method cannot unambiguously discern the effect of fusion protein. On the basis of this, we have developed a classification system based on observations of binding profiles from fluorescence polarization assay and DSF in primary screening campaigns. This scheme can be used to make decisions about what extracts/compounds to advance into subsequent stages of chemical deconvolution or lead generation. In this aspect, the selectivity of ABT-737 towards untagged Bcl-X_L was regarded as the ideal behavior, since this compound exhibited the best desired behavior in inhibitors of Bcl-2 family proteins at the hit-to-lead stage of lead identification.²⁵ Thus, we use this classification to indicate non-optimal behavior, the severity of which needs to be addressed by retesting in a different assay such as surface plasmon resonance or eliminated from further consideration. Therefore, DSF can be used as a rapid secondary assay that would facilitate the selection and prioritization of hits for characterization in other assays and/or chemical elaboration by medicinal chemists.

The selectivity of certain subsets of inhibitors such as kendomycin towards fusion Bcl-X_L could be explained by the recent report showing that GST-tag proteins tend to be dimeric,²⁴ and dimerization of Bcl-X_L had significantly increased pore forming activity in comparison to monomers.²⁶ Therefore, it is tempting to speculate that this class of inhibitors would exert effective inhibitory activity towards pore-forming activity of pre-formed Bcl-X_L dimers that were shown to express abundantly in cells.²⁷ Alternatively, the affinity tag may cause a significant conformational switch in the Bcl-X_L, thereby resulting in the selectivity for certain subsets of small molecule inhibitors. It is also plausible that the interaction of compounds with distinct sites other than the classic BH3 domain binding cleft where ABT-737 is

shown to dock may result in thermal destabilization effect on untagged Bcl-X_L.²⁸ Our finding may also suggest that ABT-737 is mechanistically different from other tested compounds, and alternative Bcl-X_L independent mechanism such as activation of other unidentified mitochondrial targets is certainly possible. Further works will be required to rigorously answer these questions.

The application of DSF in studying protein-peptide interactions has been validated and shown to correlate well with their computed binding affinity.²⁹ The binding profile results of BH3 peptides obtained from DSF were also found to be consistent with the results obtained through plasmon surface resonance and fluorescence polarization.¹⁹ However, the different effects of the fusion state on BH3 peptide versus chemical inhibitors binding may reflect specific conformational requirements for ligand binding. The subtle changes in thermal stability of BH3 peptides as compared to chemical inhibitors may raise the possibility that chemical inhibitors could induce a global change in the protein structure, whereas peptide binding may moderately remodel the Bcl-X_L hydrophobic groove compared to the monomer structure, with widening and straightening of the cleft.²⁶ As revealed by crystallographic studies, ABT-737 required a further opening-up of the binding groove beyond that required to accommodate BH3 peptidic ligands.³⁰ A similar observation was also reported in an NMR study of chelerythrine and BH3I-1.^{22,28} Therefore, this indicates that DSF serve as valuable tool that allows rapid mechanistic understanding on the binding behavior of ligands.

Although the simplicity and general applicability of DSF make the technique attractive for identification of positive hits, one should be cautious in extracting further information such as the potency ranking order and the magnitude of binding constants from the ΔT_m values. There is an assumption that the

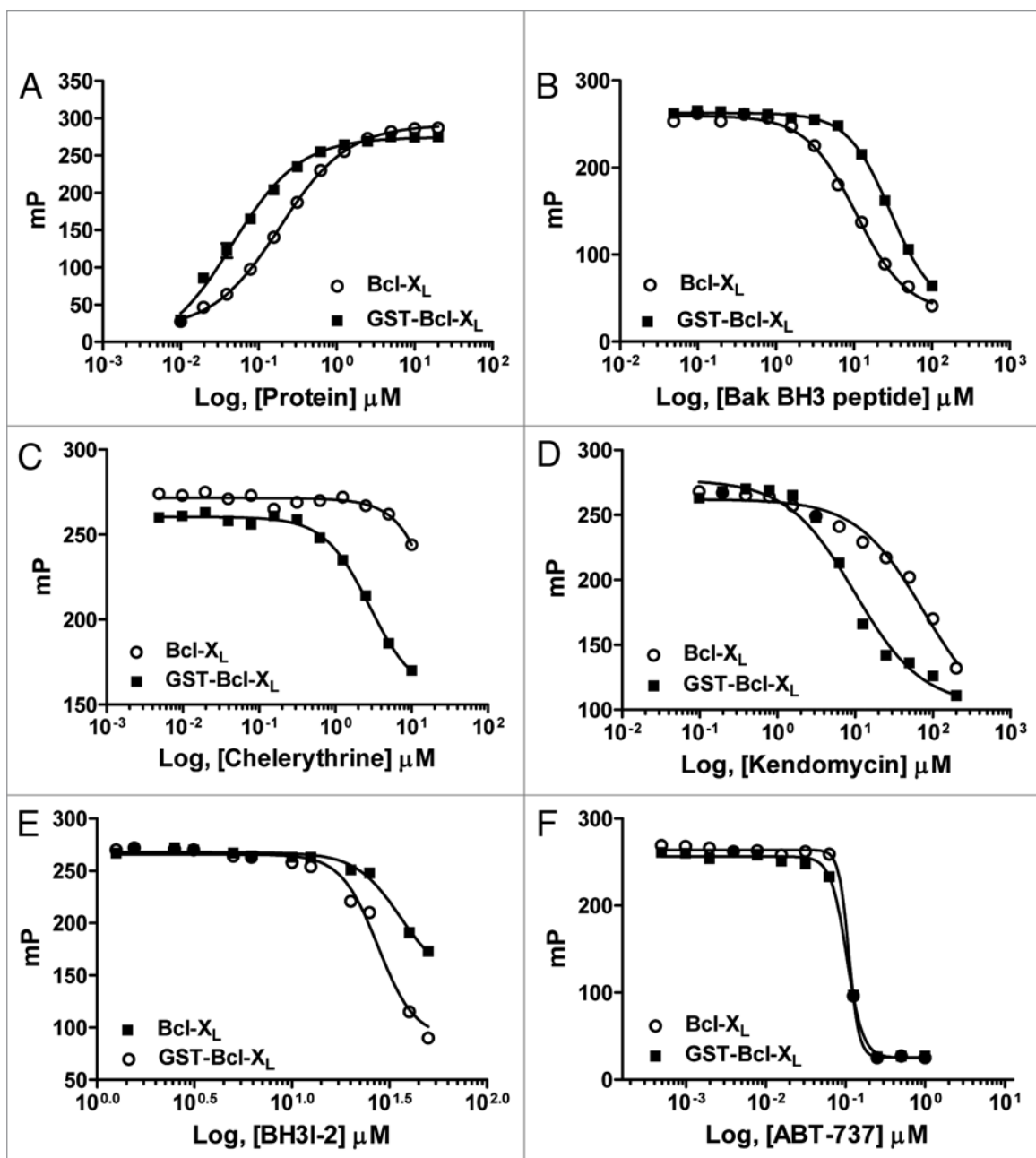


Figure 5. Fluorescence polarization analysis for known Bcl-X_L/Bcl-2 inhibitors using FAM-Bak BH3 peptide and GST-Bcl-X_L or Bcl-X_L. (A) Various concentrations of Bcl-X_L and GST-Bcl-X_L were titrated into reactions with fixed concentration of FAM-Bak BH3 peptides (60 nM). (B–F) Competitive assay analysis of 60 nM FAM-Bak BH3 peptide from 1.5 μM GST-Bcl-X_L or Bcl-X_L using various concentrations of (B) unlabelled Bak BH3 peptide; (C) chelerythrine; (D) kendomycin; (E) BH3I-2; (F) ABT-737. Data are representative of at least three experiments.

ligands bind only to the folded state with similar enthalpy. If a compound binds both the native and unfolded states of the proteins, the observed ΔT_m will be smaller leading to under estimation of the binding affinity. In addition, compounds that can bind to more than one site on a protein will appear more potent because of the additive effect on the ΔT_m values of the respective binding sites. Although this can be useful information, especially in the context of structure-based drug design, it can result in a bias in the structure-activity relationship of hits. It should also be noted that while DSF method used for comparing compound

affinity offers many advantages, results may differ somewhat if other types of binding assays are employed, such as solid-binding assays using proteins immobilized on solid supports.

Despite the limitations discussed above, DSF should be seen as secondary tool complementary to classical fluorescence polarization method of determining ligand activity. These caveats notwithstanding, the comparison of chemical inhibitors of anti-apoptotic Bcl-2 family proteins provided here offers a framework for designing experiments that utilize these compounds for drug discovery research and drug target validation. These studies

also have relevance for other screens based on the use of GST-tagged proteins and it will be important to examine this issue in the context of the widespread use of such proteins in activity based screens for example in the screening of protein kinase inhibitors.

Methods and Materials

Reagents. BH3I-1, BH3I-2, EGCG, YC-137 and HA14-1 were obtained from Calbiochem. Gossypol, chelerythrine and sanguinarine were obtained from Sigma. ABT-737 and its enantiomer were obtained from Abbott Laboratories.

Production of GST-Bcl-X_L and Bcl-X_L. The DNA sequence encoding Bcl-X_LΔC19 was inserted into the GST fusion protein vector pGEX-TK4E. The plasmid was transformed into the *Escherichia coli* strain BL 21, and the fusion protein was isolated as described previously.⁹ GST-Bcl-X_LΔ19 was eluted with 100 mM glutathione, 50 mM Tris-HCl (pH 8.0). Eluate was dialyzed against phosphate-buffered saline (PBS) containing 15% glycerol and concentrated to 1 μg/ml using Amicon centrifugal concentrating devices. The GST moiety was cleaved using thrombin protease (Sigma), and after thrombin inactivation, separated from the protein by a further chromatographic step using glutathione Sepharose 4B, followed by 5 mL HiTrap Q HP exchange column (GE healthcare) to remove the thrombin.

Fluorescence polarization assay. The Bak-BH3 peptide labeled with fluorescein at the N terminus was synthesized by Mimotopes (Clayton, Victoria, Australia) and purified by HPLC. The peptide was dissolved in DMSO at 1 mM, and stock solutions of the test compounds (10 mM in DMSO) were used for serial dilutions (100 μM to 98 nM final concentrations). The reaction was carried out in a total volume of 100 μL/well containing 1.5 μM of GST-Bcl-X_LΔC19 or untagged Bcl-X_LΔC19 and 60 nM labeled peptide in assay buffer (50 mM Tris, pH 8, 150 mM NaCl and 0.1% bovine serum albumin). To each well was added 10 μL of the test compounds, and the reaction mixture was incubated at room temperature for 1 h. The fluorescence polarization values were determined using Tecan Safire plate reader at the excitation/emission wavelengths of 485/535 nm.

Differential scanning fluorimetry. Before initiating the secondary screen, each protein was scanned to assess the suitability of the method and the lowest concentration of protein needed to generate a strong signal was determined. Compound concentrations varied between 3 μM and 100 μM, depending on the anticipated affinity and the requirement to limit the

Table 3. Summary table of IC₅₀ for known Bcl-X_L/Bcl-2 inhibitors in displacing Bak BH3 peptides from Bcl-X_L and GST-Bcl-X_L measured by FPA

Inhibitors	FPA (IC ₅₀ μM)	
	GST-Bcl-X _L	Bcl-X _L
Kendomycin	9.93	76.6
Chelerythrine	2.83	>100
YC-137	>100	>100
BH3I-1	10.63	20.45
BH3I-2	27.61	36.05
Gossypol	23.92	55.25
ABT-737	0.104	0.110
Bak BH3 peptide	29	11

concentration of DMSO to ≤2%. 20 μM of GST-Bcl-X_L and Bcl-X_L in PBS containing Sypro Orange dye (Invitrogen) and the indicated concentrations of compounds in a reaction volume of 25 μl were incubated in the wells in RT-PCR devices (BioRad iCycle5). The samples were heated at 1°C per min, from 40°C to 90°C. The fluorescence intensity was measured every 1°C. Fluorescence intensities were plotted as a function of temperature and accurate fitting to the Boltzmann equation by non linear regression was performed using GraphPad Prism. The inflection point of the transition curve T_m was calculated using Boltzmann equation, $y = LL + (UL - LL) / (1 + \exp((T_m - \chi) / a))$ where LL and UL are the values of minimum and maximum intensities, respectively, and a denotes the slope of the curve within T_m. Normalization of the RFU was also performed to prevent distraction due to different maximum and minimum values upon compounds or peptides treatment. The RFU values from different data sets were converted to a common scale (100 for UL and 0 for LL). Each DSF experiment was repeated for at least three times.

Proteolytic digestion analysis. 0.5 mg/mL GST-Bcl-X_L or Bcl-X_L in PBS was incubated with 5 μg/mL trypsin (Sigma) at 4°C in the absence or presence of indicated concentration of compounds for the indicated time. Reaction was stopped by adding loading dye, followed by SDS-PAGE and coomassie blue staining of the polyacrylamide gel.

Acknowledgements

We are grateful to Abbott Laboratories for providing ABT-737 and the enantiomer. This work was supported by the Biomedical Research Council of A*STAR (Agency for Science, Technology and Research), Singapore.

References

1. Strasser A. The role of BH3-only proteins in the immune system. *Nat Rev Immunol* 2005; 5:189-200.
2. Danial NN, Korsmeyer SJ. Cell death: critical control points. *Cell* 2004; 116:205-19.
3. Willis SN, Adams JM. Life in the balance: how BH3-only proteins induce apoptosis. *Curr Opin Cell Biol* 2005; 17:617-25.
4. Fletcher JI, Huang DC. Controlling the cell death mediators Bax and Bak: puzzles and conundrums. *Cell Cycle* 2008; 7:39-44.
5. Kitada S, Pedersen IM, Schimmer AD, Reed JC. Dysregulation of apoptosis genes in hematopoietic malignancies. *Oncogene* 2002; 21:3459-74.
6. Huang Z. Bcl-2 family proteins as targets for anticancer drug design. *Oncogene* 2000; 19:6627-31.
7. Kitada S, Leone M, Sareth S, Zhai D, Reed JC, Pellecchia M. Discovery, characterization and structure-activity relationships studies of proapoptotic polyphenols targeting B-cell lymphocyte/leukemia-2 proteins. *J Med Chem* 2003; 46:4259-64.
8. Leone M, Zhai D, Sareth S, Kitada S, Reed JC, Pellecchia M. Cancer prevention by tea polyphenols is linked to their direct inhibition of antiapoptotic Bcl-2-family proteins. *Cancer Res* 2003; 63:8118-21.
9. Chan SL, Lee MC, Tan KO, Yang LK, Lee AS, Flotow H, et al. Identification of chelerythrine as an inhibitor of Bcl-X_L function. *J Biol Chem* 2003; 278:20453-6.
10. Tzung SP, Kim KM, Basanez G, Giedt CD, Simon J, Zimmerberg J, et al. Antimycin A mimics a cell-death-inducing Bcl-2 homology domain 3. *Nat Cell Biol* 2001; 3:183-91.
11. Flack MR, Pyle RG, Mullen NM, Lorenzo B, Wu YW, Knazek RA, et al. Oral gossypol in the treatment of metastatic adrenal cancer. *J Clin Endocrinol Metab* 1993; 76:1019-24.
12. Janssen CO, Lim S, Lo EP, Wan KF, Yu VC, Lee MA, et al. Interaction of kendomycin and semi-synthetic analogues with the anti-apoptotic protein Bcl-xl. *Bioorg Med Chem Lett* 2008; 18:5771-3.

13. Oltersdorf T, Elmore SW, Shoemaker AR, Armstrong RC, Augeri DJ, Belli BA, et al. An inhibitor of Bcl-2 family proteins induces regression of solid tumours. *Nature* 2005; 435:677-81.
14. Wells JA, McClendon CL. Reaching for high-hanging fruit in drug discovery at protein-protein interfaces. *Nature* 2007; 450:1001-9.
15. Petros AM, Nettesheim DG, Wang Y, Olejniczak ET, Meadows RP, Mack J, et al. Rationale for Bcl-x_L/Bad peptide complex formation from structure, mutagenesis and biophysical studies. *Protein Sci* 2000; 9:2528-34.
16. Niesen FH, Berglund H, Vedadi M. The use of differential scanning fluorimetry to detect ligand interactions that promote protein stability. *Nat Protoc* 2007; 2:2212-21.
17. Pope AJ, Haupts UM, Moore KJ. Homogeneous fluorescence readouts for miniaturized high-throughput screening: theory and practice. *Drug Discov Today* 1999; 4:350-62.
18. Thuduppathy GR, Hill RB. Acid destabilization of the solution conformation of Bcl-x_L does not drive its pH-dependent insertion into membranes. *Protein Sci* 2006; 15:248-57.
19. Chen L, Willis SN, Wei A, Smith BJ, Fletcher JI, Hinds MG, et al. Differential targeting of pro-survival Bcl-2 proteins by their BH3-only ligands allows complementary apoptotic function. *Mol Cell* 2005; 17:393-403.
20. Real PJ, Cao Y, Wang R, Nikolovska-Coleska Z, Sanz-Ortiz J, Wang S, et al. Breast cancer cells can evade apoptosis-mediated selective killing by a novel small molecule inhibitor of Bcl-2. *Cancer Res* 2004; 64:7947-53.
21. Becattini B, Kitada S, Leone M, Monosov E, Chandler S, Zhai D, et al. Rational design and real time, in-cell detection of the proapoptotic activity of a novel compound targeting Bcl-X(L). *Chem Biol* 2004; 11:389-95.
22. Degterev A, Lugovskoy A, Cardone M, Mulley B, Wagner G, Mitchison T, et al. Identification of small-molecule inhibitors of interaction between the BH3 domain and Bcl-x_L. *Nat Cell Biol* 2001; 3:173-82.
23. Wang JL, Liu D, Zhang ZJ, Shan S, Han X, Srinivasula SM, et al. Structure-based discovery of an organic compound that binds Bcl-2 protein and induces apoptosis of tumor cells. *Proc Natl Acad Sci USA* 2000; 97:7124-9.
24. Zhai D, Jin C, Satterthwait AC, Reed JC. Comparison of chemical inhibitors of antiapoptotic Bcl-2-family proteins. *Cell Death Differ* 2006; 13:1419-21.
25. Bruncko M, Oost TK, Belli BA, Ding H, Joseph MK, Kunzer A, et al. Studies leading to potent, dual inhibitors of Bcl-2 and Bcl-x_L. *J Med Chem* 2007; 50:641-62.
26. O'Neill JW, Manion MK, Maguire B, Hockenbery DM. BCL-X_L dimerization by three-dimensional domain swapping. *J Mol Biol* 2006; 356:367-81.
27. Upreti M, Lyle CS, Skaug B, Du L, Chambers TC. Vinblastine-induced apoptosis is mediated by discrete alterations in subcellular location, oligomeric structure and activation status of specific Bcl-2 family members. *J Biol Chem* 2006; 281:15941-50.
28. Zhang YH, Bhunia A, Wan KF, Lee MC, Chan SL, Yu VC, Mok YK. Chelerythrine and sanguinarine dock at distinct sites on BclX_L that are not the classic BH3 binding cleft. *J Mol Biol* 2006; 364:536-49.
29. Madhumalar A, Lee HJ, Brown CJ, Lane D, Verma C. Design of a novel MDM2 binding peptide based on the p53 family. *Cell Cycle* 2009; 8:2828-36.
30. Lee EF, Czabotar PE, Smith BJ, Deshayes K, Zobel K, Colman PM, et al. Crystal structure of ABT-737 complexed with Bcl-x_L: implications for selectivity of antagonists of the Bcl-2 family. *Cell Death Differ* 2007; 14:1711-3.

©2009 Landes Bioscience.
Do not distribute.